76. Peptide Conformations

Part 31[1])

The Conformation of Cyclosporin A in the Crystal and in Solution

by **Hans-Rudolf Loosli**[a])*, **Horst Kessler**[b])*, **Hartmut Oschkinat**[b]), **Hans-Peter Weber**[a]), **Trevor J. Petcher**[a]), and **Armin Widmer**[a])

[a]) *Sandoz Ltd.*, Pharmaceutical Division, Preclinical Research, CH-4002 Basle
[b]) Institut für Organische Chemie der J.-W.-Goethe-Universität Frankfurt, Niederurseler Hang, D-6000 Frankfurt 50

(30.XI.84)

The all-light-atom X-ray crystal-structure analysis of cyclosporin A (**1**), a cyclic undecapeptide containing seven *N*-methylated amino acids, reveals a conformation very similar to that of the previously analysed iodo derivative which is characterised by a twisted β-pleated sheet involving the residues Me-Val-11, MeBmt-1, Abu-2, Sar-3, MeLeu-4, Val-5, MeLeu-6, and Ala-7. The β-bend at Sar-MeLeu-4 is of type II', and the loop of the residual amino acids involves a cis-peptide bond between MeLeu-9 and MeLeu-10. The NH proton of D-Ala-8 closes a γ^i-bend with a H-bond to the MeLeu-6 CO group. The crystal was grown from acetone. A closely similar backbone conformation in apolar solvents such as $CDCl_3$ or C_6D_6 has been derived from the interpretation of the NMR spectral parameters (homo- and heteronuclear NOE effects, coupling constants, chemical-shift values of the C-, H-, and N-atoms). A minor variation in the backbone conformation between crystal and solution is observed in the region of D-Ala-8, where in solution a 3-center H-bond is established between the NH of D-Ala-8 und the carbonyl O-atoms of both MeLeu-6 (γ^i-turn) and D-Ala-8 (C_5-bend). A recently proposed technique to identify intramolecular H-bond *via* heteronuclear NOE from NH proton to carbonyl C-atoms is critically analysed. The main difference between crystal and solution conformations lies in the orientation of the side chains of the unusual amino acid MeBmt ($\chi_1 = +60°$ in solution, $-168°$ in the crystal) and of MeLeu-10 ($\chi_1 = -60°$ in solution, $+60°$ in the crystal). The differences in crystal and solution are caused by the break of the intermolecular H-bond of the OH group of MeBmt on dissolution of the crystal. The bifurcated H-bond of D-Ala-8 twists the backbone in this region. Molecular modeling demonstrates that this is the origin of the change in the side chain conformation of MeLeu-10. The intramolecular flexibility in the crystal indicated by the thermal parameters obtained from the X-ray refinement, and in solution by an analysis of spin-lattice relaxation times in the NMR experiments, indicate a fairly rigid backbone and fixed conformations for all the side chains except for that of Abu-2 and the distal atoms of MeBmt.

1. Introduction. – A prerequisite for understanding drug-receptor interactions is a detailed knowledge of drug conformation [1b]. Weak intermolecular interactions such as solvent effects or crystal packing can change the observed conformation of the drug. The binding of drug to receptor can also change the conformation of the drug, the receptor, or both; but these interactions are not currently amenable to experimental observation. Thus only a careful comparison of the structure in the crystal and in solution [2], as well as in different solvents, is capable of giving us a reliable picture of the molecular flexibility of one partner in this interaction. We present here the results of our study of the potent immunosuppressive drug cyclosporin A (**1**) [3] in the crystal and in lipophilic solvents such as $CDCl_3$ and C_6D_6. In the polar solvent DMSO, a complex mixture of different

[1]) Part 30: [1a].

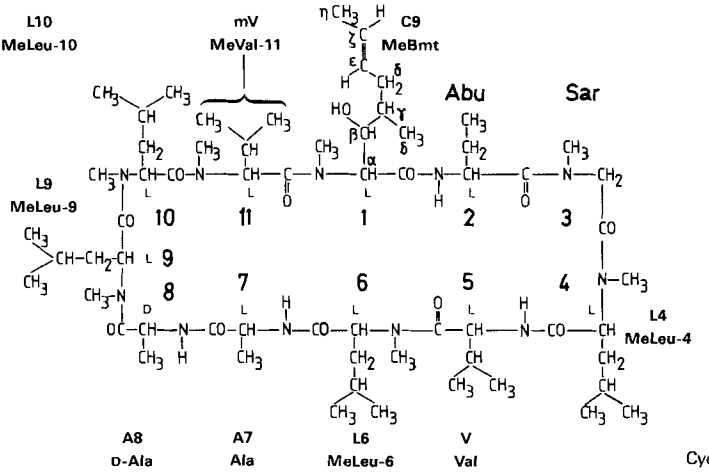

Cyclosporin A (**1**)[a])

[a]) In order to facilitate the inscriptions in the *Figures*, the amino-acid residues were abbreviated either by their conventional IUPAC/IUB three-letter notations or by more arbitrary one-letter notations which are not always in accordance with the IUPAC/IUB recommendations, *i.e.* MeBmt = **C9** (see [2]), MeLeu = **L**, Val = **V**, D- and L-Ala = **A**, MeVal = **mV**. Moreover Sar (= sarcosine) means *N*-methylglycine.

conformations is observed with interconversion rates slow in terms of the NMR time scale.

2. The Crystalline Structure of Cyclosporin A (1). – The conformation of **1** observed in the crystal is shown in *Fig. 1* with 50%-probability vibrational ellipsoids of the atomic thermal motion [4] which display the relatively small, isotopic vibrations of the backbone atoms – indicating conformational rigidity – in contrast to the more flexible side-chain

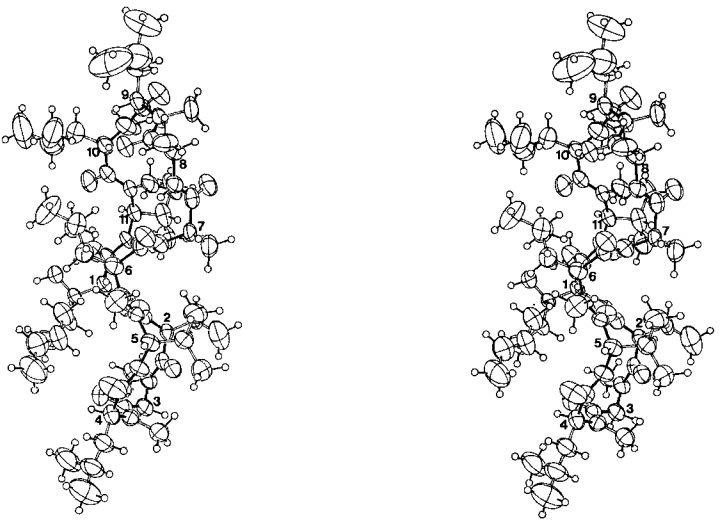

Fig. 1. *ORTEP drawing of the crystal structure of cyclosporin A* (**1**). Anisotropic atomic vibrations are represented by 50%-probability ellipsoids. The numbers shown are residue numbers.

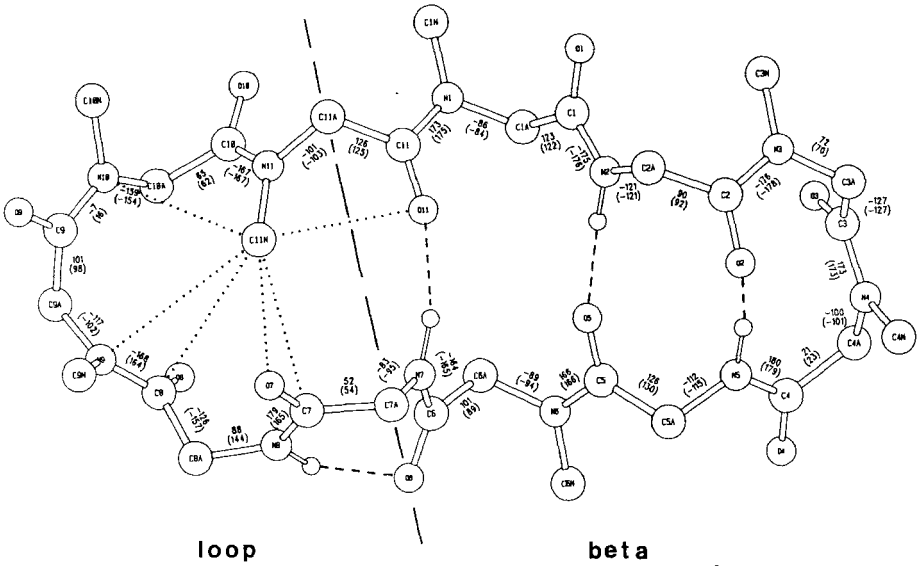

Fig. 2. *Backbone conformation of crystalline* **1** *with indication of the* loop- *and β-fragment*[3]). The torsion angles ϕ, ψ, *and* ω and in brackets the computer-modeled values for the NMR conformation are given. The dashed lines indicate H-bonds, the dotted lines close contacts from CH_3N of MeVal to different atoms (O11: 3.04 Å; C7: 3.36 Å; O7: 3.26 Å; C8: 3.41 Å; N9: 3.54 Å; N10: 3.12 Å).

atoms whose vibrational amplitudes increase with the distance from C(α). *Fig. 2* shows the backbone of the cyclic peptide with the ϕ-, ψ-, and ω-angles and some structural features. The ϕ- and ψ-angles are also summarized in a *Ramachandran* plot *(Fig. 3)*, which shows that all (ϕ,ψ)-values lie in the β-region allowed for L-amino acids[2]) with the exception of the (ϕ,ψ)-value for Sar-3, for which there is no such restriction [6], and of D-Ala-8, which, however, is in the (ϕ,ψ)-space accessible to D-amino acids only. As indicated in *Fig. 2*, the cyclic peptide can be divided into two structurally distinct moieties: (*i*) A *β-fragment*, consisting of residues 11→7, which form an antiparallel β-pleated sheet with a type-II′ β-turn [7] at residues 3→4. Three H-bonds bridge the two short β-strands (dimensions see *Table 1*), adding to the stability of the fragment. The twist in the β-sheet is right-handed, as indicated by the virtual torsion angle N5..C2..N2..C5 of +12°[3]).

Table 1. *Hydrogen Bonds in Crystalline* **1**[3])

Atoms	$d_{D...A}$	$d_{H...O}$	∢ (D–H...A)	∢ (C=O...H)
N2–H...O5[a])	2.85 Å	1.84 Å	173°	162°
N5–H...O2[a])	3.02 Å	2.06 Å	155°	119°
N7–H...O11[a])	2.89 Å	1.98 Å	162°	165°
N8–H...O6[a])	2.96 Å	1.95 Å	152°	97°
Oiβ–H...O9[b])	2.80 Å	1.87 Å	(180°)	151°

[a]) Intramolecular H-bond, H-atom constructed with N–H = 1.02 Å.
[b]) Intermolecular H-bond, H-atom constructed on the line Oiβ...O9, O–H = 0.95 Å.

[2]) MeBmt is (4*R*)-4-((*E*)-2-butenyl)-4,*N*-dimethyl-L-threonine [5].
[3]) Symbolism: the number following an atom refers to the amino-acid residue; thus, C1 = *C*O, O1 = C*O*, C1A = C(α), N1 = *N*–C(α), C1N = *C*H_3N, and Oiβ = *O*H–C(β) of MeBmt-1. H8 means NH of D-Ala-8.

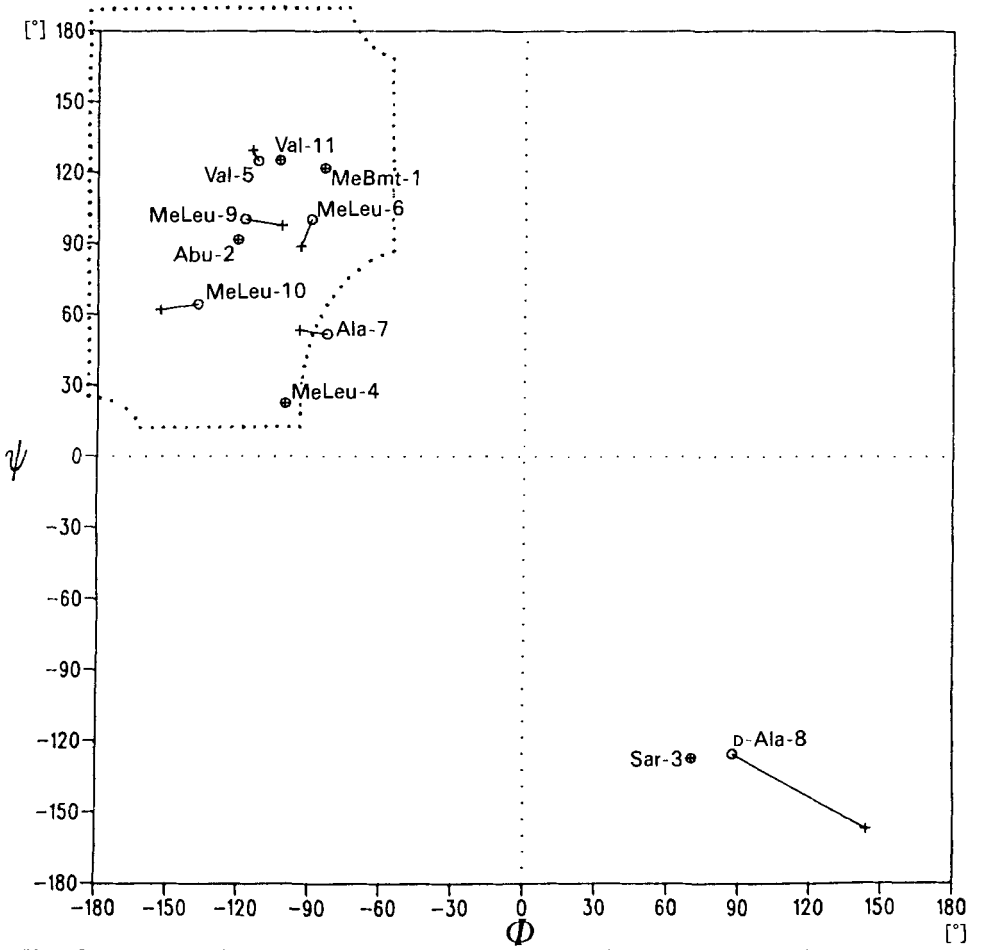

Fig. 3. Ramachandran *diagram of the solid-state conformation* (o) *and the computer-generated conformation of* **1** *in apolar solvent* (+). The β-region allowed for L-amino-acid residues is indicated.

(*ii*) Residues 7→11 form the second fragment, *the loop,* which contains several interesting features: firstly, the fourth intramolecular H-bond N8-H..O6, is part of a seven-membered ring whose conformation was predicted by *Pullman* [8] and termed C_7^{eq}, and that has also been observed in tight γ-turns in proteins [9–12]. Secondly, there is a D-amino acid in position 8 (D-Ala-8), and thirdly, there is a *cis*-amide bond between residues 9 and 10. Another remarkable feature is the position of C11N, which projects into the center of the loop fragment and makes a number of close contacts to backbone atoms. The rôle of this methyl group for the shape and stability of the loop is obvious from *Fig. 2.*

The side chains of the Abu, Val, and MeLeu residues are in the staggered conformation, the MeLeu side chains being extended. Rather unexpected is the conformation of the C_8-alkylene side chain of MeBmt-1; it is neatly folded into the ply of the β-pleated sheet which allows the molecule to adopt a globular compact shape *(Fig. 4)*. A summary of the χ-torsion angles is given in *Table 2.*

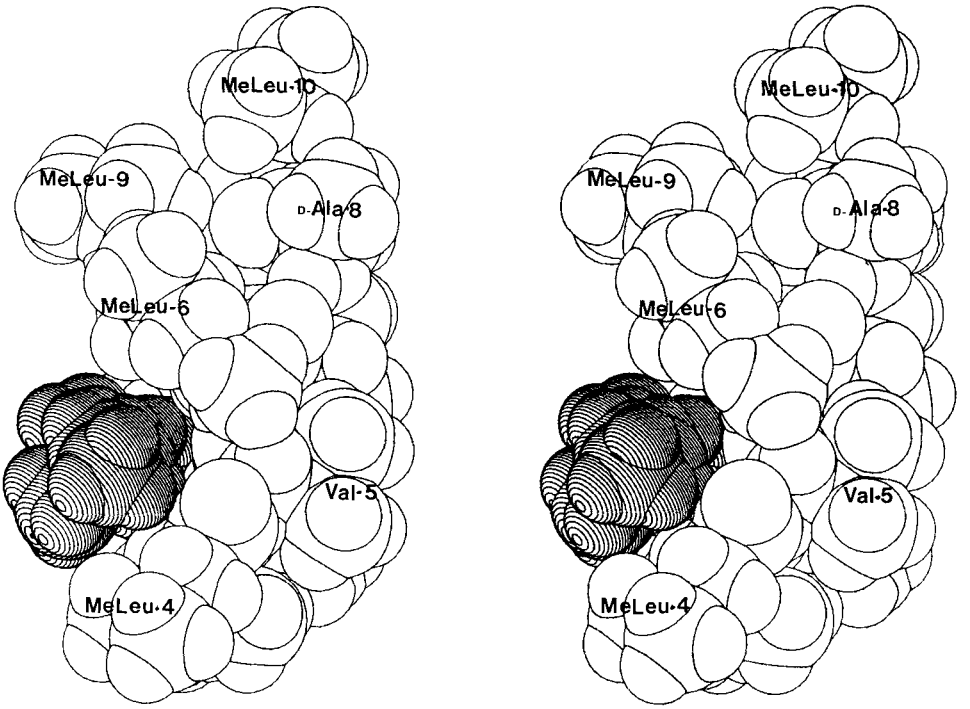

Fig. 4. *Stereoview of a space-filling model of the crystal conformation of* **1** *showing the side chain of MeBmt-1 (shaded) folded between MeLeu-6 and MeLeu-4 into the ply of the β-fragment*

It is interesting to compare the present structure to the result of an earlier X-ray analysis of a cyclosporin-A derivative, in which the C_8-side chain of MeBmt-1 was synthetically cyclised to a iodo-tetrahydrofuran [13]. In spite of the considerable chemical difference in amino acid 1, and in spite of a completely different packing in the crystal, the backbone conformations and most of the side-chain conformations of the two molecules are identical within a few tenths of an Å. This conformational similarity in two different crystal structures can be considered as evidence for a relative high *internal* stability of the molecule against intermolecular forces.

Table 2. *χ-Angles* [°] *in the Crystalline Conformation of* **1**

Residue number	Amino acid	χ^1	χ^2	χ^3	χ^4	χ^5
1	MeBmt	–168	77	–178	–128	–178
2	Abu	–178	–	–	–	–
3	Sar	–	–	–	–	–
4	MeLeu	–52	–178/–51	–	–	–
5	Val	–174/–51	–	–	–	–
6	MeLeu	–178	–178/58	–	–	–
7	D-Ala	–	–	–	–	–
8	D-Ala	–	–	–	–	–
9	MeLeu	–58	172/–59			
10	MeLeu	–165	–167/73	–	–	–
11	MeVal	–178/–51	–	–	–	–

The crystal packing of **1** is rather loose, as is indicated by the low density (1.042 $g \cdot cm^{-3}$) of the crystal. There is in fact only one strong intermolecular interaction in the crystal, *i.e.* a H-bond from the OH-group (O1β)[3]) of the MeBmt side chain to a carbonyl O-atom, O9 (see *Table 1*). All other intermolecular contacts are in the range of normal *Van der Waals* distances. There is a somewhat vague indication in the electron density that there are two solvent molecules in the crystal, possibly H_2O, but from neither of their positions it would be possible to construct a H-bond or an other strong interaction to the molecules. For crystallographic details, see *Exper. Part.*

3. Solution Conformation of 1. – Determination of conformation in solution is a complicated task. This results from the flexibility of molecules (which raises the principal problem of discussing *the* conformation), but also from the fact that methods for structure determination in solution are less direct than X-ray crystal-structure analysis. The conformational dependence of the NMR parameters delivers the most reliable information about the structure in solution, provided that an unambiguous assignment to molecular constitution is possible [1b]. We have shown in the preceding paper [1a] that modern two-dimensional techniques enable a complete assignment of all C-, all H-, and some of the N-signals in the NMR spectra of cyclosporin A.

The conformational conclusions below are based on the following experiments and NMR parameters: (*i*) Dissolution of crystals at low temperature to correlate the X-ray and solution structures; (*ii*) NOE measurements of many protons; (*iii*) discussion of vicinal coupling constants and their temperature dependence (to NH protons); (*iv*) discussion of chemical-shift values which contain information about H-bonding (δ_{CO}, δ_N), about orientation of CO groups (δ_H) as well as steric hindrance (δ_C, δ_H); (*v*) heteronuclear NOE effects from NH proton to CO groups; (*vi*) dynamic information has been obtained from longitudinal relaxation times T_1.

It is well known that in such a molecule rotations about all bonds except those of the amide bonds are fast on the NMR time scale. Also one can expect regions which differ in

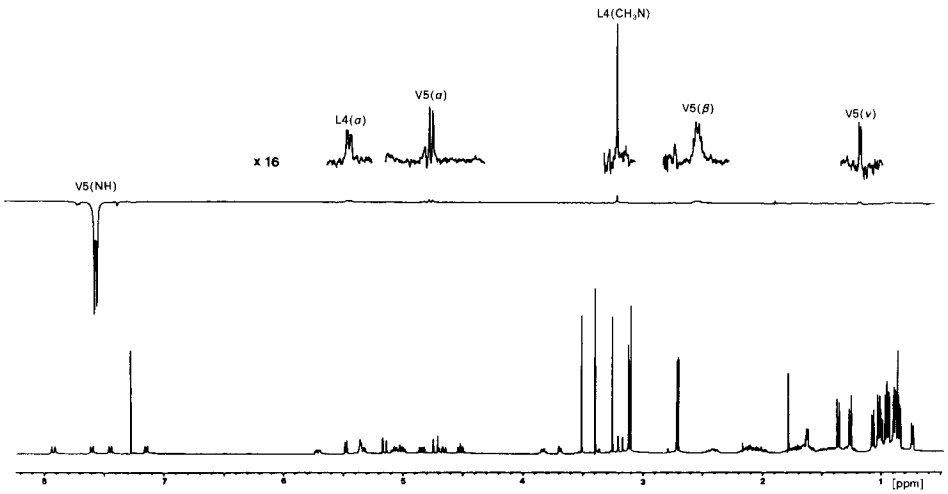

Fig. 5. *^{1}H-NMR-NOE-Difference spectrum (360 MHz) of* **1** *at room temperature in $CDCl_3$*[5]). Irradiated is N*H* of Val-5. Five distinguished NOE effects are observable.

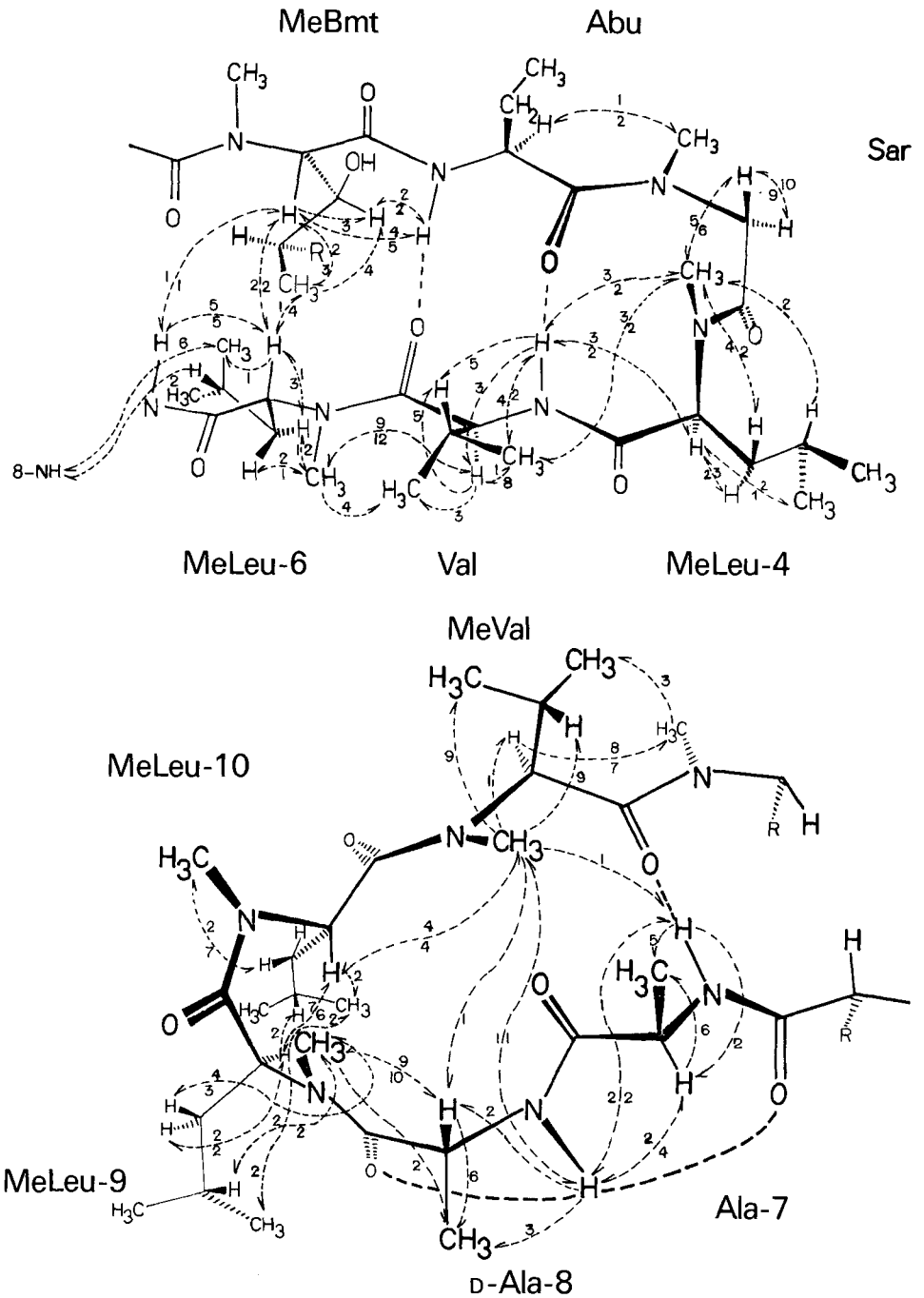

Fig. 6. *Homonuclear ^{1}H-NMR-NOE effects of* **1** *in $CDCl_3$.* The numbers are given in percent. They are arranged so that the arrow points from the irradiated proton to that which exhibits the NOE effect. A $\xrightarrow{4}$ B means irradiation in A, produces a NOE of 4% on nucleus B[5]).

their flexibility. The discussion of just one conformation in that respect means that among the conformational ensemble one conformation dominates the equilibrium. Criteria for conformational homogeneity have been described [1b].

The results on **1** (see below) point to a strong preference of one conformation of the backbone and most side chains.

3.1. *Backbone Conformation.* 3.1.1. cis/trans-*Isomerism about Amide Bonds.* Seven *N*-methylamide bonds ($N(CH_3)$–CO) give rise to the possibility of the occurrence of many *cis/trans*-conformers which interconvert slowly on the NMR time scale. In apolar solvents ($CDCl_3$, C_6D_6, CD_2Cl_2), only one conformation is populated to an extent of about 95%[4]). C-chemical-shift parameters and NOE effects give evidence that the conformation in $CDCl_3$ and CD_2Cl_2 is similar. Dissolution of crystals at −60° in CD_2Cl_2 yields the same ^{1}H-NMR spectrum as a sample cooled down from room temperature in the same solvent. The spectrum in CD_2Cl_2 is nearly identical in every respect to those measured in $CDCl_3$. Hence it is reasonable to assume a similar conformation in both solvents. CD_2Cl_2 was used as solvent because of its lower melting point. The barrier to *cis/trans* isomerism about peptide bonds (about 18 kcal/mol) [14] [15] does not allow a rotation around this bond at −60 °C. We and others have often used this procedure to correlate X-ray structures with solution structures [2] [16–19]. The results show that only the peptide bond between MeLeu-9 and MeLeu-10 is in the *cis*-conformation in the most stable conformation in solution. Independent evidence is provided by 1- and 2-dimensional NOE measurements. An example of a ^{1}H-NMR-NOE-difference spectrum is shown in *Fig. 5*. Val-5(N*H*)[5]) was irradiated. All NOE effects are positive; spin diffusion can therefore be excluded as origin of the signal enhancements. All NOE effects are summarized in *Fig. 6*. The only NOE effect between α-protons of adjacent amino-acid residues is observed for MeLeu-9 and MeLeu-10 indicating a *cis* peptide bond. At every other amide bond, a NOE effect between N*H* or NCH_3 and the α-proton of the preceding amino acid is observed *(Fig. 6)*. This confirms their *trans*-conformation. One-dimensional ^{1}H-NMR-NOE-difference spectra were performed to quantify the NOE effects. These experiments have the additional advantage that small effects can be detected. On the other hand, the resolution of 2-dimensional spectra is higher and was used in some cases to differentiate the effects observed in the 1D spectra to the specific sites. For instance, irradiation of both MeLeu-10(CH_3N) and MeVal-11(CH_3N) yields an NOE effect on MeLeu-10(*H*–C(α))[5]). In the 2D-NOE spectrum it was possible to identify this effect as resulting from MeVal-11(CH_3N). The reverse effect in a NOE-difference spectrum irradiating MeLeu-10(H–C(α)) yields additional evidence.

3.1.2. *Hydrogen Bonding.* In DMSO solution, temperature dependence of N*H* chemical shifts has frequently been used to identify external or internal NH orientations [1b] [20]. In $CDCl_3$ the effects are less clear because association effects may cause additional problems [21]. On the other hand, in rigid cyclic peptides a correspondence between orientation and temperature gradients has been observed [22] [23].

In **1** the N*H* signals of Abu, Val and D-Ala-8 are almost temperature-independent in the range from 216 to 310 K. No significant dependence of α-proton chemical shifts was observed in this temperature range. Only the Ala-7(N*H*) is shifted to high field by about

[4]) Determined by integration of the ^{1}H-NMR spectrum of the CH_3N resonances.

[5]) For notation of H- and C-atoms, see *Footnote 2* in [1a]. Here, H-atoms in the text are given in full. The meant atoms are printed in italics.

Table 3. *Temperature Dependence of the Chemical Shifts and Coupling Constants of the 4 NH Protons of* **1** *in* $CDCl_3$

	δ (216 K) [ppm]	$\Delta\delta/T$ (216 K–256 K) $10^{-3}\cdot$[ppm/K]	$\Delta\delta/T$ (300 K–310 K) $10^{-3}\cdot$[ppm/K]	$^3J_{HN,HC(\alpha)}$ (213 K) [Hz]	$^3J_{HN,HC(\alpha)}$ (298 K) [Hz]
Abu-2	8.20	1.4	0.7	8.6	9.4
Ala-7	8.28	9.7	0.5	6.0	8.0
Val-5	7.54	0.7	0.3	7.6	8.0
D-Ala-8	7.22	0.7	0.3	6.8	8.0

0.01 ppm/K in the range 216 K to 256 K. Although the usual interpretation would point to an external orientation, this result does not correspond with other information, which indicates that all 4 NH groups are involved in internal H-bridges at room temperature. Interestingly the plot of δ_{NH} *vs.* T deviates from linearity, and in the high-temperature region (296 to 310 K) the NH gradients of all NH protons are similar and relatively small. This would mean that at higher temperatures the intramolecular H-bonds are stronger and that the molecule adopts more the conformation of an isolated rather than solvated molecule. Additional support comes from the vicinal $HN,HC(\alpha)$ coupling constants which all increase with increasing temperatures *(Table 3)*. Large coupling constants are

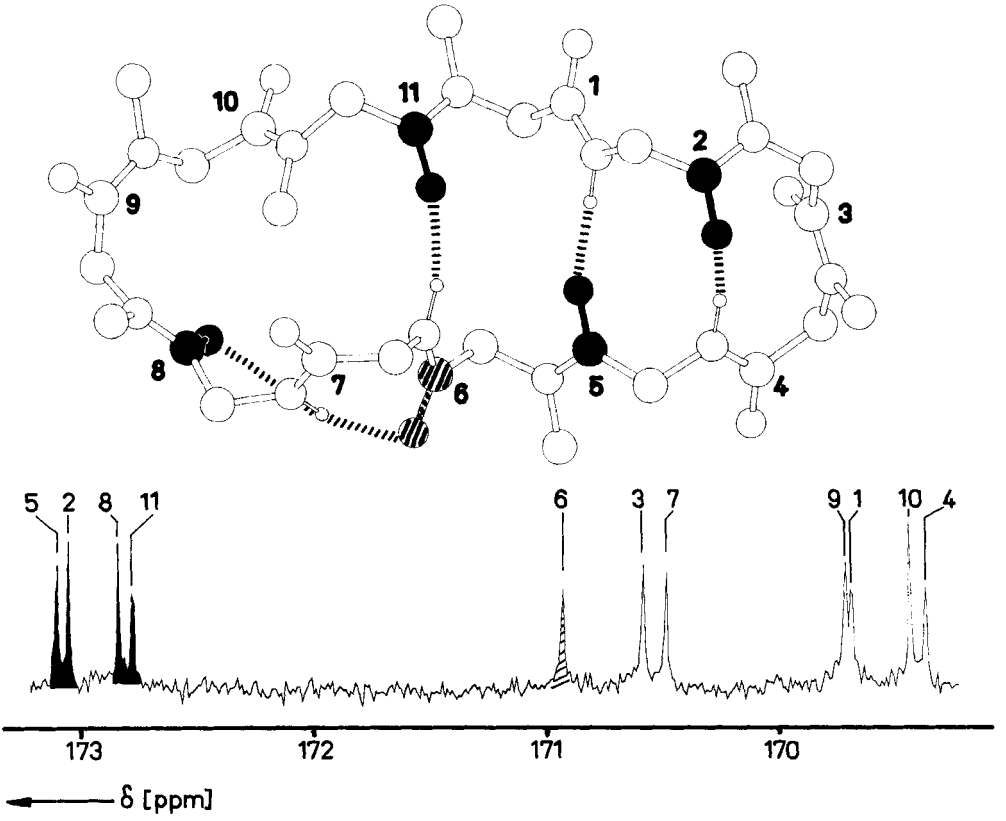

Fig. 7. *^{13}C-NMR spectrum of* **1***: CO region.* Those CO groups whose signals are shifted downfield are marked in black. The CO signal of residue 6 (shaded) is lowest from those attached to NH groups (residues 1, 4, 6, and 7).

expected for a structure similar to a β-pleated sheet. Coupling constants of 10 to 11 Hz are expected at Abu-2 and Val-5 using the dihedral angles of the X-ray structure ($\theta = 179.5°$ for Abu-2; $\theta = -172.2°$ for Val-5), whereas those of Ala and D-Ala should be somewhat smaller (9–10 Hz; $\theta = -148.0$ for Ala-7 and $\theta = 149.0$ for D-Ala-8). The data for our proposed solution structure (see below) do not significantly differ from the values given above. We interpret the destabilization of this conformation at low temperature by stronger solvation by $CDCl_3$. The entropy effect associated with solvation results in the destabilization of external deuterium bridges at higher temperatures. Hence, the tendency of the 4 NH groups to form intramolecular bridges increases. Similar effects in the stabilization of *less-solvated* molecules at *higher temperatures* have been observed and extensively discussed in the equilibrium between ions, ion pairs, and covalent molecules [24].

It should be mentioned that the IR spectra in solution also indicate that all NH groups are involved in H-bonds. Their absorption bands (3330, 3290 cm^{-1}) are independent of the concentration in the range of $4 \cdot 10^{-2}$ to $4 \cdot 10^{-4}$M in CCl_4 solution.

Having evidence that all 4 NH protons are involved in intramolecular H-bonding, the question arises which CO group acts as acceptor group. Avoiding changes of the medium (TFE addition or titration with radicals) we know 3 ways in which to obtain such information: chemical-shift effects on carbonyl C- and amide N-signals [1b] [25–27], and heteronuclear NOE effects from selectively irradiated NH protons to *C*O's [28]. Although *C*O's of ketones undergo strong downfield shifts when involved in H-bonds [29], *C*O groups of amides are less sensitive to such effects[6]). Furthermore, there is not enough experience with reliably assigned CO groups in rigid peptides. In **1** 4 *C*O groups (Abu-2, Val-5, D-Ala-8, and MeVal-11) are significantly deshielded (172.8–173.1 ppm, *Fig. 7*). Three of these CO groups (except D-Ala-8) are expected to be involved in bridges assuming the β-pleated sheet structure which is found in the solid state (see above). Hence, we suppose that the downfield shift of the *C*O groups is caused by H-bonding, especially if they are not part of a secondary amide bond (CONH). The downfield shift of D-Ala-8(*C*O) would then result from a H-bridge to its own N*H* forming a C_5-bend. So far only limited experimental evidence for such structure exists [30] [31]. In the *X-ray* structure the D-Ala-8(N*H*) is involved in a H-bond to MeLeu-6(*C*O) forming a C_7^{eq} structure (inverse γ-turn, γ^i). The distance of N*H* to *C*O of D-Ala-8 in the *X-ray* structure is 2.95 Å, whereas the distance to *C*O of MeLeu-6 is 2.00 Å. A γ-bend, in our argumentation, would cause a downfield shift of MeLeu-6(*C*O). However, this signal (dashed in *Fig. 7*) is not found in the downfield region of the 4 *C*O signals around 173 ppm, but it appears at the lowest field of all *C*ONH groups which are not *N*-methyl-substituted. The H-bond of Ala-7(N*H*) to MeVal-11(C*O*) might induce a high-field shift of the *C*O signal of MeLeu-6 which compensates partially the downfield shift induced by the γ^i-bend MeLeu-6(CO)/D-Ala-8(NH). Further insight is delivered by the N-chemical shifts. Unfortunately only the N-atoms of the NH groups have been assigned *via* ^1H,^{15}N-COSY, thus the chemical shift of the MeLeu-9(CH_3N) cannot be discussed here, but the ^{15}N-NMR spectrum in $CDCl_3$ as well as in C_6D_6 shows one of the *N*H signals strongly shifted downfield. This was assigned to Ala-7(*N*H) [1a] [32], of which the adjacent CO is the acceptor of the H-bond from D-Ala-8 (γ^i-turn). This finding, together with the ^{13}C-NMR

[6]) It is generally found that with increasing donor ability at a substituted CO group protonation induces smaller down-field shifts, whereas the protonation of CO groups yields highfield shifts instead.

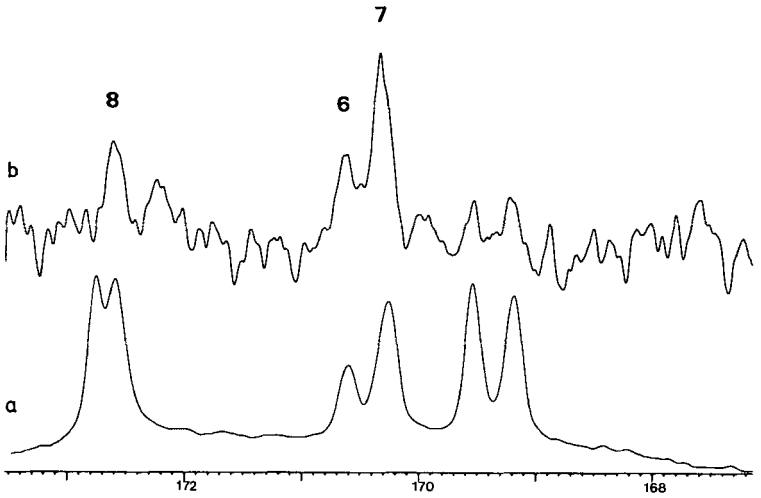

Fig. 8. a) *Fully coupled ^{13}C-NMR signals of CO groups in $CDCl_3$ and* b) *NOE-difference spectrum, obtained by irradiating* D-*Ala-8(NH) of* **1**. Beginning from low field, 3 NOE effects to *CO*'s are visible: D-Ala-8/MeVal-11, MeLeu-6, Sar-3/Ala-7. Molecular distances exclude the possibility of NOE effects to MeVal-11 and Sar-3; hence the observed effects have to be assigned to D-Ala-8, MeLeu-6, and Ala-7.

shift data, indicates that the γ^L-bend to MeLeu-6(CO) and the C_5-bend to D-Ala-8(CO) are equally possible, either as simultaneous NH bridges to both CO groups or as a rapid equilibrium between them.

The heteronuclear NOE effect [28] from D-Ala-8(N*H*) to the *CO*'s was determined *via* a NOE-difference measurement *(Fig. 8)*. A strong NOE was observed to the *CO* attached to that NH group (Ala-7(*CO*); distance N*H*...O*C* 2.1 Å). In the crystal structure, the NH of D-Ala-8 has as other near neighbors the *CO*'s of MeLeu-6 (2.5 Å) and its own *CO* (2.9 Å). And indeed, we find in solution in addition to the NOE effect on Ala-7(*CO*), smaller (20–30% of the major effect) but practically equally intense effects on the above-mentioned neighboring *CO*'s. Using the effect between the N*H* of D-Ala-8 and the *CO* of Ala-7 as an internal standard, together with the r^{-6} dependence, we can estimate that these additionally affected *CO*'s lie between 2.4 and 2.6 Å from the irradiated proton (D-Ala-8(N*H*). This is further evidence for the postulated spatial proximity in solution of D-Ala-8(N*H*) to *both* MeLeu-6(CO) and D-Ala-8(CO) in contrast to the X-ray structure (distance D-Ala-8(N*H*,*C*O) 2.9 Å).

We do not, however, consider such NOE measurements to be a generally applicable method for the localization of H-bonds [28]. Normally, linear H-bonds involve distances of about 3 Å between H and *CO*. Often distances to other neighboring *CO*'s are significantly smaller than that value. For instance the distances of Val-5(N*H*) to neighboring *CO*'s obtained from the X-ray analysis are as follows: MeLeu-4, 2.01 Å; Sar-3, 2,53 Å; Abu-2, 2.89 Å (H-bridge!); Val-5, 2.89 Å. In fact, upon irradiation of Val-5(N*H*) only a NOE to MeLeu-4(*CO*) is observed. The r^{-6} dependence of dipolar relaxation can cause only minor effects on the other *CO*'s, which do not significantly exceed the signal/noise level. Similar results are obtained from N*H* irradiation of Abu-2 and Ala-7. Our criticism of the method results from the problem in getting a sufficient signal/noise ratio for measuring distances of about ≥ 2.9 Å in those heteronuclear NOE spectra.

3.1.3. *Additional Information about the Backbone.* The confirmation that (*i*) the H-bonds and (*ii*) the *cis*-amide bond between residues 9 and 10 found in the X-ray crystal-structure analysis are also present in solution yields already a fairly good idea of the backbone conformation. For the more detailed conformation we analyzed the homonuclear NOE effects, some coupling constants, and chemical shifts of H- and C-signals.

The chirality of the amino acids involved in the β-bend allow a type-I (all L-amino acids) or a type-II' conformation (sequence LDLL) [7]. This is based on the general experience that a Gly (Sar) residue can occupy the position of a D- or L-amino acid. Only

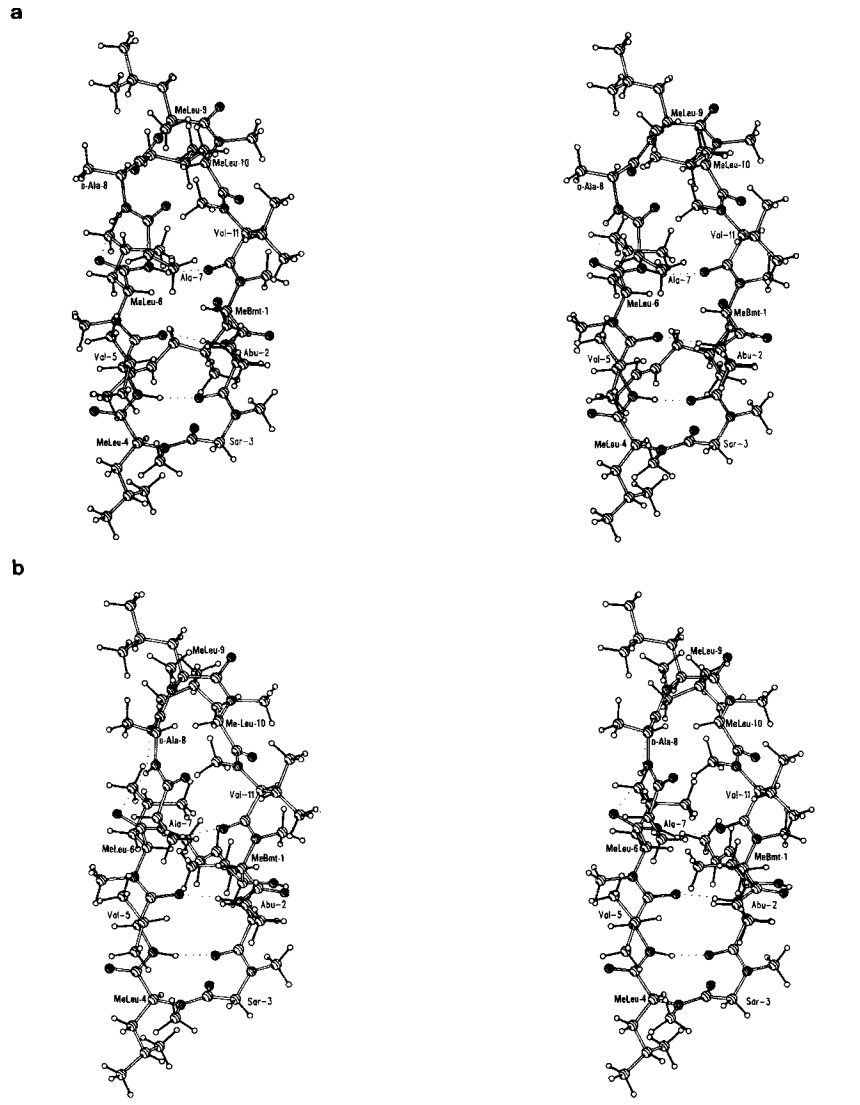

Fig. 9. *Stereoview of* **1**. a) Solid-state conformation, b) computer-generated conformation in apolar solvents (in solution the distal atoms of Abu-2 and MeBmt-1 have a high flexibility).

a type-II' β-bend is in agreement with the observed NOE effect from MeLeu-4(CH_3N) to Val-5(NH), which indicates that both groups point in the same direction (above the approximate plane, *Fig. 6*). The NOE between MeLeu-4(CH_3N) and the low field α-proton of Sar-3 assigns the signal of the latter to the (pro-*S*)-position. This α-proton points into the deshielding region of the CO group of Abu-2. The relatively small NOE between Val-5(NH) and MeLeu-4(H-C(α)) agrees with the proposed βII'-bend, which was also found in the solid state (see above). The MeLeu-4($H-C(\alpha)$) resonates at rather low field because of coplanarity to the CO group of Sar.

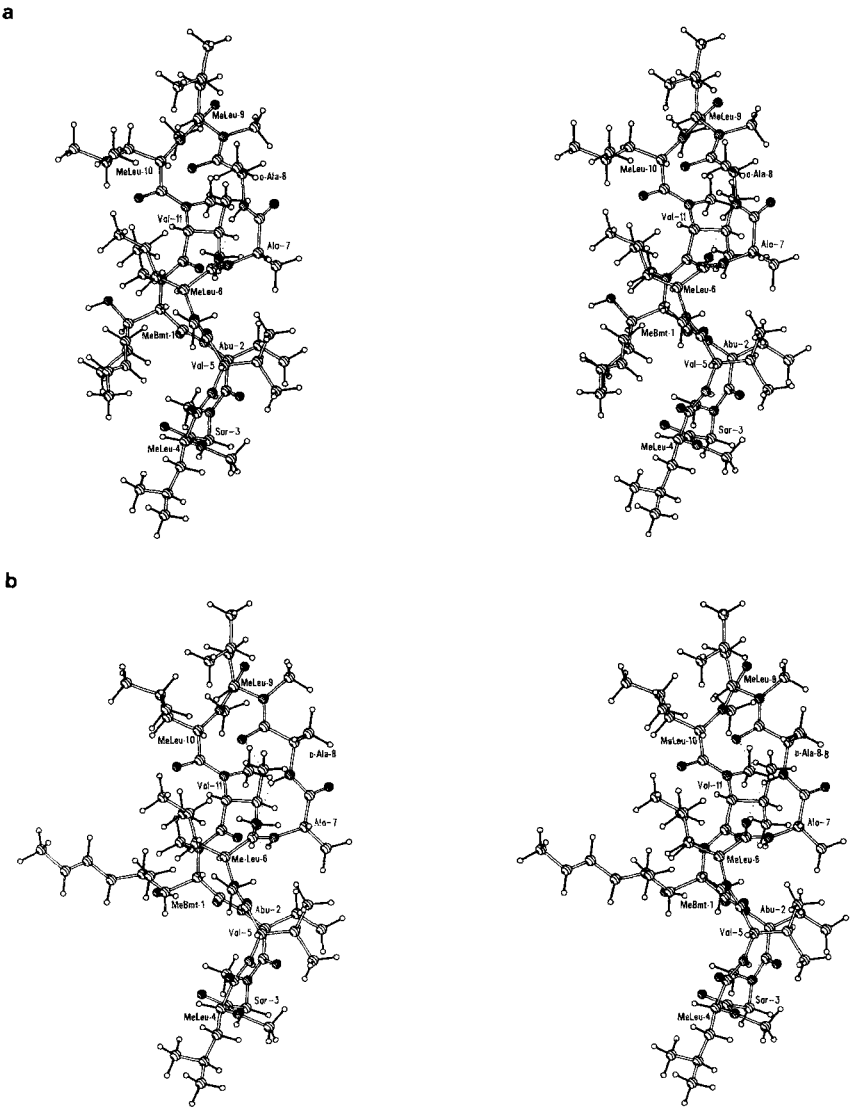

Fig. 10. *Stereoview of* **1** *approximately perpendicular to Fig. 9.* a) Solid-state conformation, b) computer-generated conformation in apolar solvents (the distal atoms of Abu-2 and MeBmt-1 have in solution a high flexibility).

The NOE effect from MeLeu-4(CH_3N) and the low-field $CH_3(\gamma)$ of Val-5 (pro-*S*) gives independent support of the βII' bend: both groups are located above the approximate ring plane. Also a βI-turn would fit this observation, but then the (pro-*R*)-proton of Sar (which does not exhibit the NOE effect to MeLeu-4(CH_3N)) would suffer the downfield shift from the CO group.

The vicinal $HN,C(\alpha)H$ coupling (J = 8 Hz) for the Val-5 residue *(Table 3)* would more or less be expected for a β-pleated sheet (see above) [33]. The strong NOE effect between Val-5($H-C(\alpha)$) and MeLeu-6(CH_3N) results from their eclipsed arrangement. Both $HN,C(\alpha)H$ couplings of Ala-7 and D-Ala-8 (J = 8 Hz) do not significantly deviate from the proposed, almost antiperiplanar arrangement of the protons (*Fig. 9* and *10*). This observation gives evidence for the quasi-equatorial position of Ala-7($CH_3(\beta)$) and is therefore in agreement with the known L-chirality of Ala-7. Hence, a configurational assignment can be performed during the course of a conformational analysis. Analoguous arguments exclude the possibility of a L-configuration of amino-acid residue 8 considering the observed NOE effects, coupling constants, and steric hindrance in molecular models. The strong NOE from D-Ala-8($H-C(\alpha)$) to MeLeu-9(CH_3N) confirms their spatial neighborhood. The unusual downfield shift of MeLeu-9($H-C(\alpha)$) may be caused by the CO group of D-Ala-8 in combination with steric effects of the *cisoid* MeLeu-10 residue. The steric effect is also expressed in the relative high-field shift of MeLeu-9($C(\alpha)$). On the other hand, MeLeu-10, surprisingly, does not exhibit a significant high-field shift of its $C(\alpha)$ signal caused by steric effects[7]). The neighboring CO orientation (ψ-angle) might induce a strong $C(\alpha)$-chemical-shift effect, but we do not know of a quantitative relationship. A mutual transannular NOE from MeBmt($H-C(\alpha)$) and MeLeu-($H-C(\alpha)$) is worth mentioning and supports the β-pleated sheet conformation.

3.1.4. *Conclusions about the Backbone Conformation.* It seems that the backbone conformation derived from the NMR parameters is very similar to the X-ray structure: (*i*) A β-pleated sheet involving a βII'-bend about Abu-2 to Val-5 is built up *via* 3 H-bridges. (*ii*) The residual amino acids contain a *cis*-peptide bond between MeLeu-9 and MeLeu-10. (*iii*) The only difference between X-ray and solution is found about D-Ala-8. NMR evidence is provided for a simultaneous formation of a C_5-structure in addition to the γ^i-bend of D-Ala-8(NH) *(Fig. 7)*.

A recent survey [34] of 1509 NH···O=C H-bonds observed by X-ray or neutron-diffraction studies has described the statistical distribution of the geometrical parameters of H-bonds, including 3-centre (bifurcated) H-bonds. A further publication [35] suggests that particularly in H-deficient amino-acid structures, a tendency to the formation of 3-centre H-bonds may be observed. Cyclosporin A with seven *N*-methylated amino acids has a structure in which there are not enough active protons (only 1 OH and 4 NH) to satisfy the normal H-bonding requirements of the candidate acceptor groups (11 carbonyl O-atoms). This molecule is therefore a typical example of that class where the formation of 3-centre H-bonds might be expected. In particular, the formation of the triad between D-Ala-8(NH), MeLeu-6(CO) and D-Ala-8(CO) would nicely explain our observations.

With the aid of molecular modeling we have been able to generate a backbone conformation that fulfils the requirements for a three-centre H-bond D-Ala-8(CO)···D-

[7]) The origin of long-range substituent effects on ^{13}C-NMR chemical shifts is still in discussion, see *e.g.* [29] and ref. cit. therein.

Ala-8(N*H*)···MeLeu-6(C*O*). The conformational search program, which was specifically developed for the purpose, minimizes the sum-of-squares of violations of a set of geometric restrictions as described below through systematic changes of a given set of torsion angles. Starting from the X-ray coordinates (with modified conformations of the side-chains of residue MeBmt-1 and MeLeu-10; see below) we have varied the backbone torsion angles of the segment Val-5 to MeLeu-10 until all of the following constraints, derived from the statistical distributions of the geometrical parameters of H-bonds mentioned above, were satisfied: O···H distances for the postulated H-bonds are restricted to the intervall 1.8 to 2.3 Å; O–H–N angles must be greater than 120° for the 3 2-centre H-bonds (90° for the 3-centre H-bond); angles C6–O6–H8 and C8–O8–H8[3]) are required to be obtuse; ψ-angles are allowed to deviate at most 15° from the ideal *trans*- or *cis*-conformations. Conformations with unfavourable *Van der Waals* contacts were excluded by placing appropriate lower bounds on distances between non-bonded pairs of atoms. All bond length and bond angles were kept at the values observed in the X-ray structure. The resulting conformation is shown in *Fig. 9* and *10*. The changes in torsion angles necessary to correspond to our interpretation of the NMR data are given in the *Ramachandran* diagram *(Fig. 3)*.

In the calculated structure, the distances from D-Ala-8(N*H*) to the 2 neighboring O-atoms (MeLeu-6(C*O*), D-Ala-8(C*O*)) are both around 2.3 Å with the H *ca.* 0.1 Å above the plane N8–O6–O8[3]). Furthermore, the angles N8–H8–O6 (139°) and N8–H8–O8 (96°) lie within the previously described statistical limits. The distances from D-Ala-8(N*H*) to the 2 neighboring *CO*'s turn out both to be 2.6 Å, in agreement with the observed heteronuclear NOE enhancements *(Fig. 8)*.

We thus are able with some conviction to postulate that the computer-generated backbone conformation very probably represents the most highly populated conformer of cyclosporin A (**1**) in an apolar environment.

3.2 *Side-Chain Conformations.* Rotation about C–C bonds of the side chains are fast with respect to the NMR time scale. Differentiation of chemical shifts of diastereotopic protons as well as of their coupling constants are used to propose the most populated rotamers in the equilibrium. Also coupling constants which deviate significantly from the mean value of approximately 7 Hz indicate preferred conformations. We shall first consider the Val and MeVal isopropyl groups. The coupling constants of 10 Hz (Val-5)

Table 4. *Assignments of the Diastereotopic Methyl Groups and Methylene Protons of the Val and MeLeu Residues of* **1** *in* $CDCl_3$

Amino acid	Methylene protons[a]) δ_H [ppm]		Methyl protons δ_H [ppm]		Methyl C-atoms δ_C [ppm]	
	pro-R	*pro-S*	*pro-R*	*pro-S*	*pro-R*	*pro-S*
Val-5			0.90	1.06	18.48	19.81
Val-11			1.01	0.86	18.79	20.26
MeLeu-4	1.64 (12)	2.00 (4.5)	0.95	0.88	23.49	21.18
MeLeu-6	1.41 (6)	2.06 (9)	0.85	0.94	21.93	23.87
MeLeu-9	2.13 (11)	1.25 (4.5)	0.97	0.89	23.74	21.86
MeLeu-10	2.13 (8)	1.24 (6.5)	0.98		23.85/23.38[b])	

[a]) In brackets: $J_{\alpha,\beta}$ [Hz].
[b]) Not assigned.

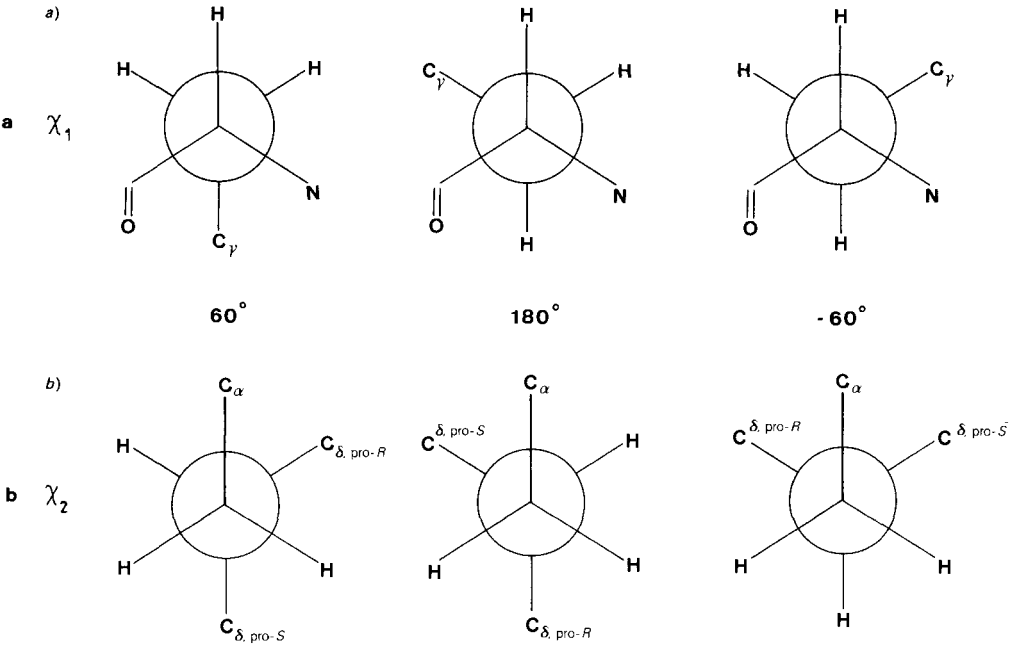

Fig. 11. Newman *projections for different torsion angles in MeLeu* a) $\chi_1(N{-}C(\alpha){-}C(\beta){-}C(\gamma))$ *and* b) $\chi_2(C(\alpha){-}C(\beta){-}C(\gamma){-}C(\delta,$ pro-R$)$

and 11 Hz (MeVal-11) indicate the antiperiplanar arrangement of the α- and β-protons in both amino-acid residues. The NOE effects *(Fig. 6)* from neighboring CH_3N groups can now be used to assign the diastereotopic methyl groups of Val and MeVal *(Table 4)*.

The conformation of the MeLeu side chain is determined by χ_1(N–C(α)–C(β)–C(γ)) and χ_2(C(α)–C(β)–C(γ)–C(δ, *pro-R*) [36]. Considering the 3 possible staggered conformations about C(α)–C(β), that with $\chi_1 = +60°$ *(Fig. 11a)* would lead to 2 small α,β-coupling constants of *ca.* 3.5 Hz. The sum of these 2 coupling constants is about 7 Hz, while the corresponding sum for the other 2 possible staggered conformations each with one antiperiplanar arrangement, (*J ca.* 12 Hz) would be *ca.* 15 Hz. We find for all 4 MeLeu the sum of the $J_{\alpha,\beta}$'s to be *ca.* 15 Hz, so we can exclude conformations with $\chi_1 = +60°$ from contributing in any major way to the conformational ensemble. This finding conforms to the expectation that $\chi_1 = +60°$ is disfavored energetically for steric reasons. The NOE effects from MeLeu(H–C(γ) and H–C(δ)) to more distant protons show whether the distal end of the side chain is in the neighborhood of its own amino group ($\chi_1 = -60°$) or of its own CO group ($\chi_1 = 180°$). Since we have not yet determined the $J_{\beta,\gamma}$'s, we have used these NOE effects to determine both χ_2 and to assign the diastereotopic $CH_3(\delta)$'s. NOE effects have also been used to assign the diastereotopic β-protons, but chemical-shift effects induced by CO groups also yield the assignments.

MeLeu-4: The NOE effect from H–C(γ) to CH_3 within MeLeu-4 show that the side chain is aligned in this direction ($\chi_1 = -60°$). A sufficiently close approach of these protons is only possible, when $\chi_1 = -60°$ *and* $\chi_2 = 180°$. The NOE effect from H–C(α) to the high-field $CH_3(\delta)$ of MeLeu-4 strongly supports a synclinal arrangement of the two and thus assigns this as the (pro-*S*)-$CH_3(\delta)$ *(Table 4)*. In this conformation, which

corresponds to that observed in the X-ray structure, the (*pro-S*)-H of $CH_2(\beta)$ lies in the plane of the CO group and is thus shifted to lower field (*Table 4*). The appropriate torsion angle O–C–C(α)–C(β), taken from the calculated structure (*Fig. 9b* and *10b*) is $-26°$. The thus assigned (*pro-S*)-H exhibits the smaller coupling ($J = 4.5$ Hz) to the α-proton. The (*pro-R*)-H of $CH_2(\beta)$ exhibits a NOE effect (2 and 4%, resp.) to CH_3N.

MeLeu-6: The NOE effect from H–C(γ) to D-Ala-8(NH) shows that the side chain points in this direction; thus χ_1 is most likely 180°. The NOE effects from the high-field $CH_3(\delta)$ to D-Ala-8(NH) and to MeLeu-6(H–C(α)) give a χ_2 of +60° and allow these to be assigned to the (*pro-R*)-$CH_3(\delta)$. In contrast to MeLeu-4, the $CH_2(\beta)$ proton which is antiperiplanar to the α-proton experiences a shift to lower field from its own CO group (τ(O–C–C(α)–C(β)) = +36°) and thus has the greater of the 2 coupling constants ($J_{\alpha,\beta} = 9$ Hz).

MeLeu-9: In an analogous manner, the NOE effects between H–C and MeLeu-9(CH_3N) indicate that the side chain is folded towards D-Ala-8 ($\chi_1 = -60°$, $\chi_2 = 180°$). Here as in MeLeu-4, the high-field $CH_3(\delta)$ may be assigned as (*pro-S*) because of the NOE effects between this $CH_3(\delta)$ and H–C(α). The $CH_2(\beta)$ proton which is shifted to lower fields by the CO group is here the (*pro-R*)-H, which is antiperiplanar to the α-proton ($J_{\alpha,\beta} = 11$ Hz, τ(O–C–C(α)–C(β)) = +36°).

MeLeu-10: In contrast to the 3 previously discussed MeLeu's, the 2 $J_{\alpha,\beta}$'s are both not larger than 8 Hz (6.5 and 8 Hz). The sum of the coupling constants is a bit smaller than for the other MeLeu's. This might result from a small participation of the energetically disfavored conformation with $\chi_1 = 60°$ in the equilibrium (see above). Since the chemical shifts for the β-protons are markedly different, it is not possible that second order effects are here leading to a deceptively simple spectrum. Further, the clear NOE effect from MeLeu-9(H–C(α)) to MeLeu-10(H–C(γ)) argues against a mixture of χ_1-rotamers in approximately equal amounts and speaks rather for a preferred χ_1 of *ca.* −60° and χ_2 of *ca.* 180°. We explain, therefore, the relative similarity of the $J_{\alpha,\beta}$'s by a deviation from the ideally staggered conformation. This conclusion is supported by the still relatively large sum of the two coupling constants (14.5 Hz) in connection to the strong non-equivalence of the β-proton shifts. The (*pro-R*)-H is antiperiplanar to H–C(α) and is shifted to low field. Since both $CH_3(\delta)$'s have the same chemical shift, further assignment is not possible. The side-chain conformation of MeLeu-10 ($\chi_1 = -60$) is different from that in the crystal ($\chi_1 \approx -165°$). Both conformations are in the energetically favored range ($\chi_1 = 180°$ or −60°), but we cannot find a simple reason for the difference. A possible explanation for this difference might, however, be the following: we noted that when we modified the X-ray backbone conformation in such a manner as to attain bifurcated H-bonding from D-Ala-8(NH) to the 2 CO of MeLeu-6 and D-Ala-8, the C(δ)'s of MeLeu-6 and MeLeu-10 approached closer to each other than the sum of the *Van der Waals* radii. Thus a conformational change in one or the other side chain is necessary to accomodate the backbone conformation observed in solution. It appears that it is the MeLeu-10 side chain which rotates by 120° about the C(α)–C(β) bond as a result of the backbone change.

The assignment of the diastereotopic $CH_3(\delta)$'s of MeLeu-4, MeLeu-6, and MeLeu-9 can be checked using their C-chemical-shift values. Recently it has been pointed out [37] that the CH_3's of isopropyl groups can be differentiated because the synclinal (= *gauche*) CH_3 exhibits a high-field shift. In fact, the (*pro-S*)-C(δ) of MeLeu-4 and MeLeu-9 as well

as the (*pro-R*)-C(δ) of MeLeu-6 which are *gauche* to the C(α)–C(β) bond are shifted to higher field (*Table 4*).

Both β-protons of Abu-2 exhibit similar chemical shifts. No significant NOE effect to Abu($CH_3(\gamma)$) was observed. Together with the high flexibility of this residue (derived from T_1-measurements, see below) we consider that the rotamers are similarly populated.

One of the most interesting features of the NMR interpretation is the side-chain conformation of MeBmt. The relatively small $J_{\alpha,\beta}$ (5.7 Hz) together with NOE effects from MeBmt (H–C(β)) to Abu-2(NH) and a small, but significant transannular NOE of MeBmt($CH_3(\delta)$) to MeLeu-6(H–C(α)) results in a conformation shown in *Fig. 9b* and *10b* ($\chi_1 = +60°$, $\chi_2 = +60°$). The IR-absorbtion band of the OH group (3500 cm^{-1}) is

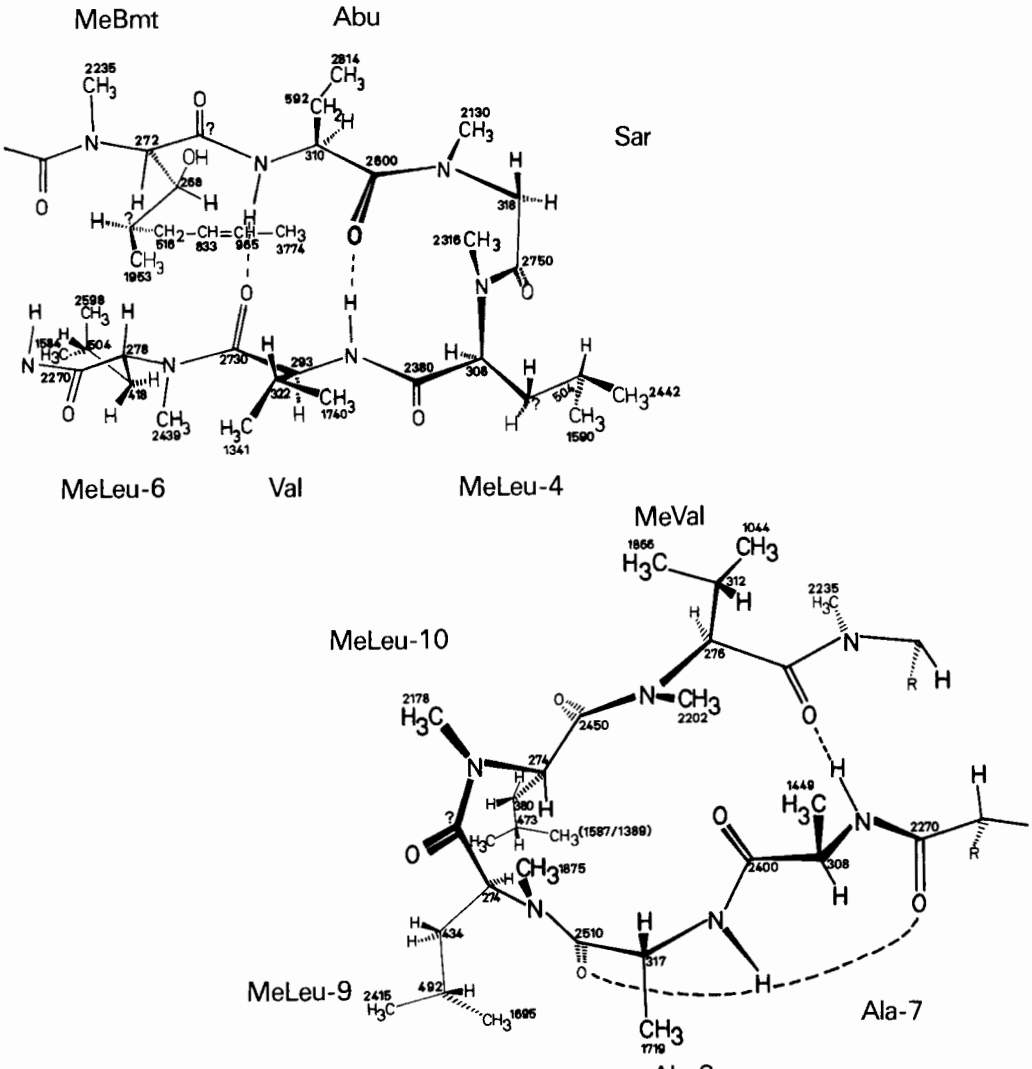

Fig. 12. NT_1-*Values [ms] for the C-atoms of* **1** *in* $CDCl_3$

concentration-independent in the range of $4 \cdot 10^{-2}$ to $4 \cdot 10^{-4}$M in CCl_4 solution. This indicates that the OH group forms an intramolecular H-bridge. Thus the side-chain conformation of MeBmt is in clear contrast to the X-ray structure (*Fig. 9a* and *10a*). The increasing flexibility along the side chain indicated by the T_1 values (see below) excludes a meaningful interpretation of the further chain conformation of MeBmt.

3.3. *Molecular Flexibility.* To obtain information about molecular flexibility, we determined the spin-lattice relaxation times T_1 of all C-atoms. Under the assumption of a dipolar relaxation mechanism and isotopic molecular tumbling, the NT_1 values (N = number of attached protons at each C-atom) yield information about motions at the order of the *Larmor* frequencies [38] [39]. In flexible molecules internal mobility adds to the overall tumbling rate of the molecule. Hence, increasing NT_1 values indicate regional mobility in the molecule[8]).

The NT_1 values of the C-atoms *(Fig. 12)* are similar for all backbone C-atoms of the various amino acids. We may thus assume that the entire backbone is equally flexible (or rigid). The greatest NT_1 values are found for the distal atoms of the side chains of Abu-2 and MeBmt, indicating their greater freedom of movement.

We attempted to correlate the NT_1 values with the temperature factors of the individual atoms from the X-ray crystal-structure refinement. Such a correlation has been observed in cyclic tripeptides [42] and was in accord with force-field calculations [43]. In the case of **1** we found no correlation. This may be because of the different time scales of the observations. In NMR spectroscopy only the window of spectral density around the *Larmor* frequency is used, whereas the X-ray experiment, in contrast, delivers information about the vibration of atoms about a mean position in an essentially infinitely ordered 3-dimensional array of molecules and furthermore includes statistical disorder of molecules in the crystal. Thus fine nuances in crystal-packing forces can affect the apparent intramolecular flexibility. It is also well known to most practising crystallographers that any residual systematic errors arising during the measurement of the diffracted intensities tend to migrate into the vibrational, rather than the positional, parameters during the course of the least-squares refinement.

4. Conclusions. – This, to our knowledge the first, detailed X-ray crystallographic and NMR conformational analysis of a medium-sized cyclic polypeptide has shown the following points: (*i*) The availability of a high-resolution crystal-structure analysis can be of considerable assistance in the discussion of NMR parameters with respect to molecular conformation.

(*ii*) In this instance where the molecule is highly lipophilic, the solid-state conformation and that deduced from interpretation of NMR spectra in apolar solvents are closely similar. The only differences we have found are the side-chain conformation of MeBmt (a major change between the chain folded in upon the molecule in the solid state, and pointing out into solvent in the NMR study), the side-chain conformation of MeLeu-10, and the detailed backbone conformation in the region of D-Ala-8 *(Fig. 13)*. Here the X-ray structure clearly shows *one* H-bond from D-Ala-8(N*H*) to MeLeu-6(C*O*), whereas in solution we observe a bifurcated H-bond to *both* this carbonyl O-atom *and* to the carbonyl O-atom of D-Ala-8 itself. It is of considerable interest that the conformational

[8]) Many more sophisticated models have been proposed and applied [40] [41]. We believe that such a rigorous theoretical treatment does not yield additional information for that qualitative picture.

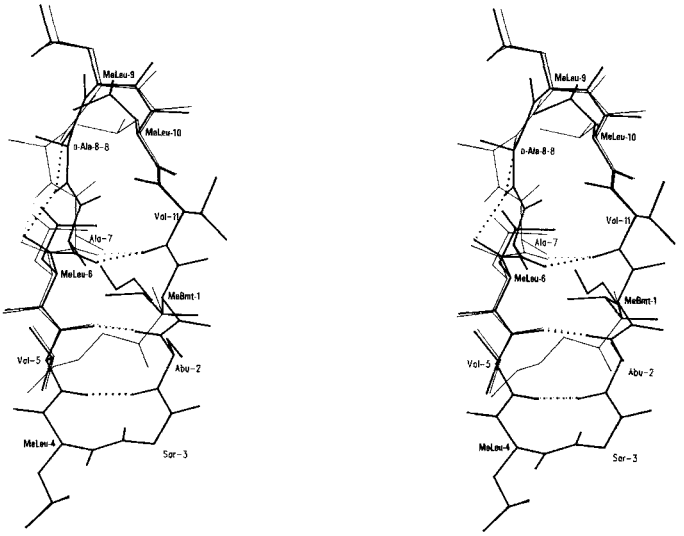

Fig. 13. *Superposition of the solid-state conformation (thin lines) and the computer-generated conformation of* **1** *in apolar solvent (thick lines)*

change needed to convert the X-ray backbone into the NMR backbone is small, and can be brought about by relatively small rotations in the backbone torsion angles in the region MeLeu-6 to MeLeu-9, principally around the 7- and 8-residues.

(*iii*) The side-chain conformations of MeVal and Val and of 3 of the 4 MeLeu-residues (MeLeu-4, MeLeu-6, MeLeu-9) are virtually identical in crystal and solution. Only that of MeLeu-10 is rotated by 120° (χ_1), probably caused by the remote backbone conformational change about residue D-Ala-8.

(*iv*) The side-chain conformation of MeBmt in solution is derived from the X-ray conformation simply by means of a 120° rotation about the α,β-bond. This rotation, which is certainly energetically allowed, could be the result from the formation of an intramolecular H-bond between the β-OH and the carbonyl O-atom of MeBmt itself, replacing the intermolecular H-bond found in the crystal. The tendency to emphasize intramolecular bridges in solution compared to intermolecular ones in the crystal is general and often explains the differences observed between conformations in crystal and solution [2] [17].

(*v*) The resulting overall molecular shape in apolar solution is that of the previously postulated 'butterfly' [13], in which the MeBmt side chain, known to be important for immunosuppressive activity, stands out, proboscis-like, in a manner suggestive of special function.

(*vi*) Whether this indeed is the conformation in which cyclosporin A (**1**) interacts with its receptors remains still to be shown. The fact that this conformer is only 95% populated in apolar medium, and that the ensemble of conformations in polar media remains inaccessible to experimental investigation is tantalising, but it has been most satisfying to see the close conformational correspondence in two states of aggregation described in this report.

Experimental Part

X-Ray Crystallography. – A summary of the crystal data and diffractometry is given in *Table 5*. During data collection, 3 control reflections were measured periodically, and a slow decay of the crystal specimen was observed. The reduction of the intensities from start to the end of diffractometry amounted to about 10%, and intensity data were accordingly scaled.

Table 5. *Crystal and Diffraction Data*

Molecular formula	$C_{62}H_{111}N_{11}O_{12}$	Molecules per cell	$Z = 4$
Molecular weight	1202.5	Diffractometer	*CAD4 (Enraf-Nonius)*
Crystallisation	from acetone	Radiation	CuK_α (Graphite Monochromator)
Crystal form	colourless, prismatic	Intensity scans	$\omega/2\theta = 1.0$; $\Delta\omega = 1.0° + 0.3 \tan\theta$
Crystal size	*ca.* 0.2 × 0.2 × 0.3 mm		$\sigma(I)/I = 0.02$ ($t_{max} = 120$ s)
Space group	$P4_1$ (No 76)	Sphere of reflexion	$\sin\theta/\lambda \leqslant 0.51$ (36508 reflexions)
Cell dimensions	$a = b = 13.837\,(2)$,	Intensities measured	5057 (unique)
	$c = 41.242\,(3)$ Å; $V = 7896$ Å^3	Intensities significant	4272 ($I \geqslant 2.5\sigma(I)$);
Crystal density (calc.)	$d_c = 1.042$ g·cm^{-3}		$\sigma(I) = \{\Sigma i_n + 0.02 \cdot I\}^{1/2}$

Geometric-data correction (not including absorption), and reduction of intensities to absolute structure factors yielded the averages: $< |E| > = 0.837$, $< |E^2 - 1| > = 0.810$, $< |E|^2 > = 0.982$, $\bar{B} = 5.2$ Å^2. The experimental error for F_o was calculated as $\sigma(F_o) = \sigma(F_o^2)/2F_o$ (for significant structure factors). The structure could be solved by application of the MULTAN program package [44]. After several unsuccessful attempts, a fragment consisting of 6 amides was vaguely outlined in a peak map, which then could be extended to the full structure by 4 successive structure-factor and electron-density calculations. Extensive refinement of the structure by block-diagonal LS procedures followed, in the course of which anisotropic temperature factors were introduced, and H-atoms were constructed in fixed theoretical positions. In an intermediate stage of the refinement, a difference electron density revelated 2 large residual peaks, which were interpreted as 'possible solvent atoms'. They were included into refinement as 2 H_2O molecules. It is interesting to note that the 2 putative H_2O molecules do not make any H-bonds or other close contacts to the peptide, and obviously just fill 'empty space'.

The weighting scheme applied in the LS procedure is $\omega = 1/\sigma(F_o)$, ($\omega = 0$ for insignificant F_o), and the refinement was terminated after 24 cycles at convergence of 767 parameters with an $R = 0.114$ for the 4272 significant structure factors, or $R = 0.136$ for all 5057 measured $|F_o|$ values.

The average positional errors for C-, N-, and O-atoms obtained from the LS procedure, are 0.021, 0.012, and 0.014 Å, resp. These e.s.d.'s appear to be realistic, since they compare well with the internal r.m.s.'s of the 11 $C^i(\alpha)$–C^i bond lengths, 0.027 Å (mean 1.515 Å), of the 10 $C^i(\alpha)$–$C^i(\beta)$, 0.030 Å (mean 1.512 Å), of the 11 $C^i(\alpha)$–N^i, 0.031 Å (mean 1.467 Å), and of the 11 C^i=O^i, 0.022 Å (mean 1.233 Å). There are only 23 significant deviations of molecular parameters from normal, expected values; (*i*) the 2 bond angles at the double bond in MeBmt-1 are opened to 132 and 133°, resp., which may, however, be an artifact due to the large anisotropy of the outer side-chain atoms, and (*ii*) in the MeLeu side chains the bond angles ($C^i(\alpha)$–$C^i(\beta)$–$C^i(\gamma)$) are consistently opened from normal 112° to *ca.* 118°. Supplementary material is available from the *Crystallographic Data Centre*, Cambridge (U.K.).

NMR Spectroscopy. – The 1-dimensional ^{1}H- and ^{13}C-NMR-NOE spectra were measured on a *Bruker-WH-360* spectrometer with an *Aspect-2000* computer. The ^{13}C T_1 measurements were carried out on a *Nicolet NT 300 WB* instrument with a *NMC-1280* computer. All measurements were performed at r.t. Concentrations: ^{1}H-NMR-NOE: 0.04M in $CDCl_3$. ^{13}C-NMR-NOE: 0.35M in $CDCl_3$. ^{13}C-NMR-T_1: 0.13M in $CDCl_3$.

Homonuclear ^{1}H-NMR Difference NOE Spectra. Size 16 K, sweep width 4800 Hz, pulse length 2 μs, decoupling power 35 L, decoupling time 0,35 s, recycling time 3.7 s, 1056 acquisitions each on-resonance and off-resonance. The intensity standard was the intensity of the Abu-2(N*H*) signal in the off-resonance spectrum as 100%.

Heteronuclear ^{13}C-NMR Difference NOE Spectra. Size 2 K, sweep width 580 Hz, pulse length 20 μs, decoupling power 24 L, decoupling time 10 s, recycling time 12 s, 5120 acquisitions each on-resonance and off-resonance, undecoupled spectra were recorded. Insert diameter 5 mm.

NOESY Spectrum in C_6D_6 at 270 MHz. Sequence: delay 1–90°-t_1-90°-delay 2-90°-t_2. Relaxation delay (delay 1): 5 s; 90°-pulse: 6.8 μs; delay 2: 350 ms; random variation; variation of delay 2: 15%; spectral range in both dimensions: 3205 Hz; size in f_2: 4096 data points; number of acquisitions: 176; 64 increments; data handling: strong pseudoecho in both dimensions, two times zerofilling in t_1; Temperature: 296 K.

T_1-*Measurements in $CDCl_3$ (except CO's)*. Sequence. Inversion-recovery with a composite 180°-pulse. Relaxation delay: 2.5 s; acquisition time: 590 ms; spectral range: 13900 Hz; 90°-pulse: 37.5 μs; values for recovery time: 10 ms, 30 ms, 60 ms, 90 ms, 150 ms, 250 ms, 400 ms, 900 ms; LB = 2 Hz. The T_1 are extracted from the peak heights as a function of the recovery delay according to [42]. Concentration: 130 mmol.

T_1-*Measurements of the CO-Signals*. Relaxation delay: 30 s, 90°-pulse: 24.5 μs; acquisition time: 1.24 s; spectra range: 1650 MHz; number of scans: 256; values for recovery-time: 10 ms, 200 ms, 800 ms, 1.5 s, 2.5 s, 3.5 s, 4.5 s; size: 4 K. All other parameters see above.

We thank *S. Mangin* and *L. Oberer* for skilled technical assistance, and Mrs. *T. Nägele* for her cooperation in the preparation of the manuscript. We gratefully acknowledge financial support from the *Deutsche Forschungsgemeinschaft* and the *Fonds der Chemischen Industrie*.

REFERENCES

[1] a) H. Kessler, H. R. Loosli, H. Oschkinat, *Helv. Chim. Acta* **1985,** *68,* 661; b) H. Kessler, *Angew. Chem.* **1982,** *94,* 509; *ibid. Int. Ed.* **1982,** *21,* 512.

[2] H. Kessler, G. Zimmermann, H. Förster, J. Engel, G. Oepen, W. S. Sheldrick, *Angew. Chem.* **1981,** *93,* 1085; *ibid. Int. Ed.* **1981,** *20,* 1053.

[3] a) A. Rüegger, M. Kuhn, H. Lichti, H. R. Loosli, R. Huguenin, C. Quiquirez, A. von Wartburg, *Helv. Chim. Acta* **1976,** *59,* 1075; b) R. Traber, M. Kuhn, H. R. Loosli, H. Lichti, A. von Wartburg, *ibid.* **1977,** *60,* 1247; c) R. Traber, M. Kuhn, H. R. Loosli, W. Pache, A. von Wartburg, *ibid.* **1977,** *60,* 1568; d) 'Cyclosporin A', Proceedings of an International Conference on Cyclosporin A, Cambridge, Sept. 1981, Elsevier Biomedical Press, Amsterdam, p. 19ff.

[4] C. K. Johnson, 1965. ORTEP, Oak Ridge National Laboratory Report ORNL-3794.

[5] R. M. Wenger, *Helv. Chim. Acta* **1983,** *66,* 2308.

[6] G. E. Schulz, R. H. Schirmer, 'Principles of Protein Structure', Springer Verlag, New York, 1978, p. 22.

[7] a) For the notation of β-turns, see *e.g.* P. Y. Chou, G. D. Fasman, *J. Mol. Biol.* **1977,** *115,* 135 and ref. [8]; b) J. A. Smith, L. C. Pease, *CRC Crit. Rev. Biochem.* **1980,** *8,* 316.

[8] B. Pullman, B. Maigret, in 'Conformation of Biological Molecules and Polymers', Eds. E. D. Bergmann and B. Pullman, Academic Press, Inc., New York, 1973, pp. 13.

[9] K. C. Chou, M. Pottle, G. Nemethy, Y. Ueda, H. A. Scheraga, *J. Mol. Biol.* **1982,** *162,* 89.

[10] G. Nemethy, M. P. Printz, *Macromolecules* **1972,** *5,* 755.

[11] B. W. Matthews, *Macromolecules* **1972,** *5,* 818.

[12] G. D. Rose, L. M. Gierasch, J. A. Smith, *Advances in Protein Chem.* **1984,** in press.

[13] T. J. Petcher, H. P. Weber, A. Rüegger, *Helv. Chim. Acta* **1976,** *59,* 1480.

[14] H. Kessler, *Angew. Chem.* **1970,** *82,* 237; *ibid. Int. Ed.* **1970,** *9,* 219.

[15] S. Sternhell, in 'Dynamic Nuclear Magnetic Resonance', Eds. L. M. Jackman and F. A. Cotton, Academic Press, New York, 1975, p. 163.

[16] K. Titlestad, *Acta Chem. Scand., Ser. B* **1975,** *B 29,* 153; *ibid.* **1976,** *30,* 753; *ibid.* **1977,** *31,* 641.

[17] J. W. Bats, H. Fuess, H. Kessler, R. Schuck, *Chem. Ber.* **1980,** *113,* 520.

[18] H. Kessler, P. Krämer, G. Krack, *Isr. J. Chem.* **1980,** *20,* 188.

[19] H. Kessler, R. Schuck, R. Siegmeier, J. W. Bats, H. Fuess, H. Förster, *Liebigs Ann. Chem.* **1983,** 231.

[20] K. Wüthrich, 'NMR in Biological Research: Peptides and Proteins', North-Holland Publ. Comp., Amsterdam, 1976.

[21] E. S. Stevens, N. Sugawara, G. M. Bonara, C. Toniolo, *J. Am. Chem. Soc.* **1980,** *102,* 7048.

[22] L. G. Pease, C. H. Nin, G. J. Zimmermann, *J. Am. Chem. Soc.* **1979,** *101,* 184.

[23] H. Kessler, H. Kogler, *Liebigs Ann. Chem.* **1983,** 316.

[24] H. Kessler, M. Feigel, *Acc. Chem. Res.* **1982,** *15,* 2.

[25] H. R. Kricheldorf, W. E. Hull, *Biopolymers* **1980,** *19,* 1103.

[26] G. E. Hawkes, E. W. Randall, W. E. Hull, O. Convert, *Biopolymers* **1980,** *19,* 1815.

[27] H. Kessler, W. Hehlein, R. Schuck, *J. Am. Chem. Soc.* **1982,** *104,* 4534.

[28] M. A. Khaled, C. L. Watkins, *J. Am. Chem. Soc.* **1983,** *105,* 3363.

[29] G. C. Levy, R. L. Lichter, G. L. Nelson, 'Carbon-13 Nuclear Magnetic Resonance Spectroscopy', Wiley Interscience, New York, 1976, Vol. 2, p. 2.

[30] C. Toniolo, *CRC Crit. Rev. Biochem.* **1980,** *9,* 1 and ref. cit. therein.
[31] G. Shoham, D.C., Rees, W.N. Lipscomb, G. Zanotti, T. Wieland, *J. Am. Chem. Soc.* **1984,** *106,* 4606; G.J. Govil, *J. Chem. Soc. (A)* **1970,** 2464.
[32] W.E. Hull, 'Two-Dimensional NMR', *Bruker Analytische Messtechnik,* 1982.
[33] V.F. Bystrov, *Progr. in NMR Spectroscopy* **1976,** *10,* 41.
[34] R. Taylor, O. Kennard, W. Versichel, *J. Am. Chem. Soc.* **1983,** *105,* 5761.
[35] R. Taylor, O. Kennard, W. Versichel, *J. Am. Chem. Soc.* **1984,** *106,* 244.
[36] IUPAC-IUP Commission on Biochemical Nomenclature, in 'Handbook of Biochemistry and Molecular Biology', Ed. G.D. Fasman, CRC Press, New York, 1976, Vol. I, pp. 59.
[37] A.E. Tonelli, F.C. Schilling, F.A. Bovey, *J. Am. Chem. Soc.* **1984,** *106,* 1157.
[38] F.W. Wehrli, T. Wirthlin, 'Interpretation of Carbon-13 NMR Spectra', Heyden, London, 1976.
[39] J.R. Lyerla, G.C. Levy, in 'Topics in Carbon-13 NMR Spectroscopy', Ed. C.G. Levy, John Wiley and Sons, New York, 1974, Vol. 1, pp. 79.
[40] G. Lipari, A. Szabo, *J. Am. Chem. Soc.* **1982,** *104,* 4546.
[41] R. Richarz, K. Nagayama, K. Wüthrich, *Biochemistry* **1980,** *19,* 5189.
[42] H. Kessler, A. Friedrich, G. Krack, W.E. Hull, 'Peptides: Synthesis-Structure-Function', Pierce Chem. Comp., Rockford, Ill., 1981, 335.
[43] F.A.A.M. De Leeuw, C. Altona, H. Kessler, W. Bermel, A. Friedrich, G. Krack, W.E. Hull, *J. Am. Chem. Soc.* **1983,** *105,* 2237.
[44] P. Main, W.E. Hull, L. Lesinger, G. Germanin, J.P. De Clerc, M.M. Woolfson, MULTAN 78, A System of Computer Programs, University of York and Louvain, 1978.